



# A differentially weighted Monte Carlo method for two-component coagulation

Haibo Zhao<sup>a,b,\*</sup>, F. Einar KrUIS<sup>b,\*\*</sup>, Chuguang Zheng<sup>a</sup>

<sup>a</sup> State Key Laboratory of Coal Combustion, Huazhong University of Science and Technology, Wuhan, 430074 Hubei, PR China

<sup>b</sup> Institute for Nanostructures and Technology (NST) and Center for Nanointegration Duisburg-Essen (CeNIDE), University of Duisburg-Essen, D-47057 Duisburg, Germany

## ARTICLE INFO

### Article history:

Received 31 December 2009

Received in revised form 6 May 2010

Accepted 24 May 2010

Available online 1 June 2010

### Keywords:

Multivariate population balance

Coagulation

Stochastic method

Weighting scheme

Statistical noise

## ABSTRACT

The direct simulation Monte Carlo (DSMC) method for population balance modeling is capable of retaining the history of each simulation particle and is thus able to deal with multivariate properties in a simple and straightforward manner. As opposed to conventional DSMC approaches that track equally weighted simulation particles, a differentially weighted Monte Carlo method is extended to simulate two-component coagulation processes and is thereby able to simulate the micromixing of the components. A new feature of the method for this bivariate population balance modeling is that it is possible to specify how the simulation particles are distributed over the compositional axis. This allows us to obtain information about particles in those regions of the size and composition distribution functions where the non-weighted MC methods place insufficient simulation particles to obtain an inaccurate solution. The new feature results in lower statistical noise for simulating two-component coagulation, which is validated by using two-component coagulation cases for which analytical solutions exist (a discrete process with sum kernel for initial monodisperse populations and a process with constant kernel for initial polydisperse populations).

© 2010 Elsevier Inc. All rights reserved.

## 1. Introduction

Multi-component coagulation<sup>1</sup> is ubiquitous in a number of fields such as aerosol dynamics [1], polymerization [2], granulation [3], nanoparticle synthesis [4], combustion [5], and atmospheric physics [6]. In this process, the aggregating particles are often inhomogeneous in composition, and the compositional distribution affects the end-use properties of the aggregates. In order to understand and control this coagulation process, it is therefore necessary to obtain the evolution of the compositional distribution within aggregates of a given size. This study only considers a two-component and non-reactive system. Although this is clearly the most basic case, it is nevertheless considered the most relevant, as the particles formed are usually solids which do not react chemically. Spatially homogeneous two-component coagulation processes are described by the following population balance equation (PBE) [7], which is an extension of Smoluchowski's equation for one-component coagulation,

\* Corresponding author at: State Key Laboratory of Coal Combustion, Huazhong University of Science and Technology, Wuhan, 430074 Hubei, PR China.

\*\* Corresponding author.

E-mail addresses: [klinsmannzhb@163.com](mailto:klinsmannzhb@163.com) (H. Zhao), [enar.kruis@uni-due.de](mailto:enar.kruis@uni-due.de) (F.E. KrUIS).

<sup>1</sup> The terms coagulation, aggregation and agglomeration are used as synonyms in this paper.

$$\frac{\partial n(v_x, v_y, t)}{\partial t} = \frac{1}{2} \int_0^{v_x} \int_0^{v_y} \beta(v_x - v'_x, v_y - v'_y, v'_x, v'_y, t) n(v_x - v'_x, v_y - v'_y, t) n(v'_x, v'_y, t) dv'_x dv'_y - n(v_x, v_y, t) \int_0^\infty \int_0^\infty \beta(v_x, v_y, v'_x, v'_y, t) n(v'_x, v'_y, t) dv'_x dv'_y, \quad (1)$$

where  $v_x$  and  $v_y$  are the volume of  $x$ -component and  $y$ -component within an aggregate having a total volume of  $v_x + v_y$  respectively;  $n(v_x, v_y, t)$  is the number density function at time  $t$  such that  $n(v_x, v_y, t)dv_x dv_y$  represents the number concentration of particles in the size range of  $x$ -component,  $v_x$  to  $v_x + dv_x$ , and the size range of  $y$ -component,  $v_y$  to  $v_y + dv_y$ ;  $\beta(v_x, v_y, v'_x, v'_y, t)$  is the coagulation rate coefficient between one particle A of state  $(v_x, v_y)$  and another particle B of state  $(v'_x, v'_y)$ . The two-component coagulation between particle A and B results in a new particle C of state  $(v_x + v'_x, v_y + v'_y)$  and the death of particle A and B.

The numerical solution of the two-component PBE still poses a number of difficulties due to the double integral and non-linear behavior of the equation. Not many methods are available in the open literature, which is in sharp contrast with the dozens of numerical methods for mono-component systems. Basically, it is possible to distinguish amongst methods of multi-component coagulation between deterministic methods, which directly calculate the double integral either through an appropriate discretization scheme or by quadrature, and stochastic methods, which directly simulate the dynamic evolution of a finite sample of particle population using Monte Carlo (MC) technique. Based on a deterministic method, Kim and Seinfeld proposed the sectional method [8] and the finite element method [9] for simulating the evolution of aerosol size and chemical composition distributions resulting from simultaneous coagulation and growth successively; McGraw and Wright [10] extended the quadrature method of moments for aerosol dynamics simulation in multi-component systems; Vale and McKenna [11] extended the fixed pivot technique of Kumar and Ramkrishna [12] to simulate two-component coagulation processes; Alexopoulos and Kiparissides [13] also used the extended fixed pivot technique for solution of a bivariate PBE considering simultaneous coagulation and breakage; Qamar and Warnecke [14] extended a conservative finite volume approach of Filbet and Laurecot [15] to determine the number density function of two-component aggregates. Generally, these deterministic methods are computationally less demanding and can be coupled with solvers of computational fluid dynamics (CFD) for the fields of continuous phase to simulate spatially-dependent multi-component coagulation. However, these deterministic methods are formulated by complicated mathematical equations, especially when simulating more than two internal variables of the particles such as the chemical composition, size, charge or surface area of aggregates, which are necessary in the simulation of, for example, multi-component nanoparticle synthesis via the gas phase method at high temperature. At the same time, the deterministic equation (1) cannot provide information regarding the innate fluctuations for multi-component coagulation [16] and, more unfortunately, may not be valid at longer time periods, when only several particles acquire a mass larger than the rest of the population [17] and complete coagulation occurs [16].

The stochastic methods, or the population balance-Monte Carlo (PB-MC) methods, have become increasingly popular in the past two decades because computer technology (especially CPU and memory) is developing rapidly and, more importantly, the discrete and stochastic nature of the PB-MC methods is especially suited for particle dynamics, which is also discrete and stochastic in nature. The PB-MC can be adopted for multivariate population balances (such as the two-component coagulation in this study) in a simple and straightforward manner. Kruijs et al. [4,18] adopted the stepwise constant volume method to track the time evolution of multivariate systems including particle size, charge and component. Saliakas et al. [19] also used the stepwise constant volume method to predict the dynamic evolution of the droplet/particle size distribution in both non-reactive liquid-liquid dispersions and reactive liquid (solid)-liquid suspension polymerization systems. Matsoukas et al. [20,21] used the constant number method to investigate the mixing and granulation of components. Sun et al. [22] developed a time-driven PB-MC to capture both composition and size of particles undergoing simultaneous coagulation and fast condensation, where particles are grouped into bins with moving boundaries according to their size. These PB-MC methods (particle accounting algorithms in the nomenclature of Laurenzi et al. [16]) for multivariate systems are direct and simple extensions of these corresponding univariate PB-MC methods. The main numerical difficulties in these multivariate PB-MC methods are that the numerical operation increases linearly as the increment of internal variable number ( $\kappa$ ), and the storage requirement is nearly proportional to  $\kappa^2$  [16]. Laurenzi et al. [16] thus designed a special MC method for multi-component coagulation processes using a chemical interpretation to define the state of an aggregating system in terms of “aggregate species”. The so-called species accounting algorithm has remarkable performance in terms of computational efficiency and memory demand thanks to the use of the bookkeeping based on an “aggregation table”. Irizarry [23] recently also viewed particles with size in a specified interval as pseudo chemical species and then constructed a jump Markov model that defines a set of non-standard reactions between pseudo-species (called random product channels). The resulting event-driven MC, point ensemble Monte Carlo in Irizarry’s nomenclature, is capable of keeping the particle integrity during simulation and describing multivariate particulate systems. The two aforementioned types of PB-MC methods (species accounting algorithms in the nomenclature of Laurenzi et al. [16]), both of which adopt the stochastic simulation algorithm for chemical kinetics [24], cut the computational requirement significantly, however, at the cost of very complicated algorithms.

In fact, these available PB-MC methods for multivariate population balance modeling in the open literature track simulation particles which are equally weighted. Even when millions of simulation particles are used in the equally weighted MC, there may still be an insufficient number of simulation particles at the edges of the compositional distributions, which makes it impossible to determine the compositional distributions in this area using MC. This becomes especially clear for multi-

component systems because the distribution functions of each component within aggregates are nonisotropic. The effective route is the differentially weighting scheme of simulation particles. Differentially weighted simulation particles can be specified to distribute as homogeneously as possible over high-dimensional joint space of internal variables, which will greatly reduce statistical noise inherent to the MC method and determine full compositional distributions in multi-component coagulation processes. We proposed a time-driven differentially weighted MC [25] and an event-driven differentially weighted MC [26] for coagulation of mono-component particles successively. In this paper, the two differentially weighted MC are unified and the generalized MC is then directly extended to simulate two-component coagulation processes, where composition-dependent weighting schemes are designed to specify the distribution of simulation particles in composition. Ideal cases in which analytical solutions exist are simulated to validate the performance of the MC.

## 2. The differentially weighted Monte Carlo method for two-component coagulation processes

### 2.1. Theoretical basis of the differentially weighted MC method

The concept of weighting simulation particles is widely utilized by MC to overcome the conflict between large numbers of real particles and limited CPU speed and memory capacity. In differentially weighted MC, the weight of a simulation particle  $i$ ,  $w_i$ , means the simulation particle  $i$  represents  $w_i$  real particles having the same or similar internal variables (i.e., size, component) as  $i$ . In order to use differentially weighted simulation particles, the coagulation rate between simulation particles having different weights must be derived.

Since a simulation particle is a representative of some real particles having similar size, one naturally considers that, once simulation particle  $i$  coagulates with another simulation particle  $j$ , each of the real particles represented by  $i$  or  $j$  undergoes a real coagulation event with 100% probability, that is, each real particle from two coagulated simulation particles must coagulate and coagulates only once. We can call the pre-established rule *the full coagulation rule*. On the basis of this rule, the total coagulation rate of simulation particle  $i$ ,  $C_i$  (with dimension  $m^{-3} \cdot s^{-1}$ ), is calculated as [27,28]:

$$C_i = \sum_{j=1, i \neq j}^{N_{st}} C_{ij}^i = \frac{1}{V^2} \sum_{j=1, i \neq j}^{N_{st}} (\beta_{ij} w_j), \tag{2}$$

where  $V$  is the volume of the simulated system;  $N_{st}$  is the total number of simulation particles in the system;  $w_i$  and  $w_j$  are the private weights of particle  $i$  with volume of  $v_i$  and particle  $j$  with volume of  $v_j$ , respectively;  $\beta_{ij}$  is the coagulation kernel between particle  $i$  and particle  $j$ ,  $m^3 \cdot s^{-1}$ ;  $C_{ij}^i$  is the coagulation rate of  $i$  for the  $i$ - $j$  coagulation event,  $C_{ij}^i = \beta_{ij} w_j / V^2$ . The time interval of  $i$  ( $\delta_{ij}^i$ ) is then  $1 / (V C_{ij}^i)$ . It is worth mentioning that, for the equally weighted simulation particles, the total coagulation rate of  $i$  is then  $C_i = \frac{w}{V^2} \sum_{j=1, i \neq j}^{N_{st}} \beta_{ij}$ , and especially, if one simulation particle represents one real particle  $C_i = \frac{1}{V^2} \sum_{j=1, i \neq j}^{N_{st}} \beta_{ij}$ . These formulas are consistent with those adopted by the stepwise constant volume method [29] and the time-driven DSMC [30].

In the full coagulation rule, the number of real coagulation events for the  $i$ - $j$  coagulation event is  $w_i \times w_j$ . Since the total number of real particles from  $i$  and  $j$  is  $(w_i + w_j)$ , and one coagulation event is related to two particles, the mean number ( $\Omega$ ) of real coagulation events per real particle from  $i$  or  $j$  is  $2w_i w_j / (w_i + w_j)$ . The average time interval per real particle from  $i$ ,  $\bar{\delta}_{ij}^i$ , is thus given by  $\bar{\delta}_{ij}^i / \Omega$ , i.e.,  $1 / (V \Omega C_{ij}^i)$ . The mean coagulation rate of a real particle from  $i$  ( $\bar{\theta}_{ij}^i$ ) is then  $1 / (V \bar{\delta}_{ij}^i) = \Omega C_{ij}^i$ .

If the full coagulation rule is utilized to construct a jump Markov process for coagulation dynamics, we are faced with the conceptual difficulty of imagining a coagulation event between two simulation particles having different weights. As for the  $i$ - $j$  coagulation where  $w_i > w_j$ , for example, real particles from  $i$  need  $w_i$  real particles from  $j$  to realize real coagulation in pairs, while real particles from  $j$  only need  $w_j$  real particles from  $i$  to match them. That is,  $(w_i - w_j)$  real particles from  $i$  are unable to find their coagulation partner from  $j$ , even though  $(w_i - w_j)$  real particles must coagulate according to the coagulation rule. Following the coagulation rule, it is difficult to design a scheme to describe the resulting simulation particle  $k$  from coagulation between  $i$  and  $j$ , where the size and weight of  $k$  should be specified to satisfy some basic laws such as mass conservation.

We further derived a new coagulation rule for coagulation events between two differentially weighted simulation particles [25], where probability theory is introduced to consider real coagulation in pairs. Under this rule, for a coagulation event between simulation particle  $i$  and  $j$ , it is imagined that each real particle from  $i$  undergoes a real coagulation event with a probability of  $\min(w_i, w_j) / w_i$ , and each real particle from  $j$  does so with a probability of  $\min(w_i, w_j) / w_j$ . Thus, on average, only  $\min(w_i, w_j)$  real particles from  $i$  or  $j$  participate in real coagulation. The  $\min(w_i, w_j)$  coagulation pairs are chosen randomly from the set of all real particles  $i$  and  $j$  respectively. We call this *the probabilistic coagulation rule*.

According to the probabilistic coagulation rule, the number of real coagulation events for the  $i$ - $j$  coagulation event is  $\Omega' = \min(w_i, w_j)$ . Similarly, the mean coagulation rate of a real particle from  $i$  ( $\bar{\theta}_{ij}^i$ ) is  $\Omega' C_{ij}^i$ , where  $C_{ij}^i$  is the coagulation rate of  $i$  for the  $i$ - $j$  coagulation event in the probabilistic coagulation rule.

Whether the full or probabilistic coagulation rule is adopted, the coagulation rate of a real particle from the same simulation particle should be the same ( $\bar{\theta}_{ij}^i = \bar{\theta}_{ij}^i$ ), that is,  $\Omega C_{ij}^i = \Omega' C_{ij}^i$ . So:

$$C_{ij}^i = \frac{\Omega}{\Omega'} C_{ij}^i = \frac{2w_i w_j}{(w_i + w_j) \times \min(w_i, w_j)} C_{ij}^i = \frac{2 \max(w_i, w_j)}{w_i + w_j} C_{ij}^i \geq C_{ij}^i. \quad (3)$$

The total coagulation rate of simulation particle  $i$  with any other simulation particles in the probabilistic coagulation rule is calculated using:

$$C_i' = \sum_{j=1, j \neq i}^{N_{st}} C_{ij}^i = \frac{1}{V^2} \sum_{j=1, j \neq i}^{N_{st}} \left[ \frac{2\beta_{ij} w_j \max(w_i, w_j)}{w_i + w_j} \right] = \frac{1}{V^2} \sum_{j=1, j \neq i}^{N_{st}} \beta'_{ij}, \quad (4)$$

where  $\beta'_{ij}$  is a normalized kernel that relates not only to the states (like volumes) but also to the weights of the two simulation particles,  $\beta'_{ij} = 2\beta_{ij} w_j \max(w_i, w_j) / (w_i + w_j)$ .

## 2.2. The generalized MC method

MC methods can be divided into two classes according to the treatment of the time step. These are referred to as “event-driven” and “time-driven” MC. In the paper, the two MC modes are generalized for the first time on the basis of the probabilistic coagulation rule. Three key issues here are the choice of time step, the selection of coagulation pairs and the treatment of a coagulation event.

### 2.2.1. The choice of time step

In event-driven MC, the time step is derived from mean-field rates of corresponding processes, i.e., the waiting time between two successive coagulation events for all simulation particles, as follows [26]:

$$\Delta t_{ED} = 2 \left/ \left( V \sum_{i=1}^{N_{st}} C_i' \right) \right. = 2V \left/ \sum_{i=1}^{N_{st}} \sum_{j=1, j \neq i}^{N_{st}} \beta'_{ij}, \right. \quad (5)$$

where the factor “2” accounts for one coagulation event involving two simulation particles. In such a way there is one event and only one event within the time step in event-driven MC.

Differently, in time-driven MC, the total number of events within a time step is generally far greater than 1, where the time step is restricted to be less than or equal to the waiting time between two successive coagulation events for a simulation particle, i.e., a simulation particle is restricted to participating in one coagulation event at most. The time step in time-driven MC is usually calculated as follows [25]:

$$\Delta t_{TD} = \alpha \left/ \max_{vi} (VC_i'), \right. \quad (6)$$

where the multiplicative factor  $\alpha$  usually has a very small value (such as 0.01) in order to ensure that several coagulation events are uncoupled within a sufficiently small time step. In the open literature,  $\alpha$  is chosen according to experience and usually has different values in different cases depending on the particulars of the problem. What is more,  $\alpha$  is generally set to a constant value during MC simulation. In fact, an increase of  $\alpha$  causes more computational expense and decreasing accuracy. For example, for initial monodispersed particles, every particle initially has the same total coagulation rate. At that moment, one must set a very small  $\alpha$  to avoid too many coagulation events occurring within the step. During the evolution of the particle population, the weight and size of simulation particles will differ increasingly. The number of particles having similar total coagulation rates thus diminishes. In this condition, it should be possible to choose a comparatively large  $\alpha$  to accelerate simulation. Up to now, there has been no known method that allows us to specify an optimal  $\alpha$  according to the actual distribution of coagulation rates of the simulation particles. In this paper, a formula to determine  $\alpha$  during dynamic evolution is proposed. It is known that the number of coagulation events within a time step should be greater than or at least equal to 1 and less than or at most equal to  $N_{st}/2$ , that is, the ratio of the number of coagulated simulation particles to the whole simulation particle number  $p$  should be between  $2/N_{st}$  and 1. If we specify this ratio  $p$  to be a constant value, then the time interval for these coagulation events with number of  $(p \times N_{st}/2)$  is  $(p \times N_{st}/2) \times \Delta t_{ED} = pN_{st} / \sum_{i=1}^{N_{st}} (VC_i')$ . We can now determine the time step in time-driven MC or the multiplicative factor  $\alpha$  in Eq. (6) as follows:

$$\Delta t_{TD} = pN_{st} \left/ \sum_{i=1}^{N_{st}} (VC_i'), \right. \quad \text{or} \quad \alpha = pN_{st} \max_{vi} (C_i') \left/ \sum_{i=1}^{N_{st}} C_i', \right. \quad (7)$$

Using Eq. (7) to determine the optimum time step, time-driven MC is capable of adjusting the time step during the dynamic evolution and avoiding the null event (like event-driven MC). It is also worth noting that no additional computational cost is caused for Eq. (7) and, although another empirical parameter  $p$  is introduced, time-driven MC can perform with good accuracy and efficiency when  $p$  is set to around 0.01 ~ 0.05. The idea can also be used in the  $\tau$ -PEMC (point ensemble Monte Carlo) method proposed by Irizarry [23] to automatically determine the so-called coarse-graining factor.

### 2.2.2. The selection of coagulation pair(s)

On the basis of the total coagulation rate of each simulation particle, a jump Markov model for particle coagulation is then constructed; that is, within a prescribed time step the interacting particle pair(s) is (are) selected with probability  $\beta'_{ij} / \sum_i \sum_{j \neq i} \beta'_{ij}$ . Either the cumulative probabilities method or the acceptance-rejection method is used to realize the jump Markov model.

In event-driven MC using the cumulative probabilities method, the first coagulated simulation particle  $i$  is determined by:

$$\frac{V\Delta t_{ED}}{2} \sum_{m=1}^{i-1} C'_m \leq r_1 \leq \frac{V\Delta t_{ED}}{2} \sum_{m=1}^i C'_m, \tag{8}$$

where  $r_1$  (and other random numbers in this paper) is a random number from an uniform distribution in the interval  $[0, 1]$ . Its coagulation partner  $j$  is then selected if the following relation:

$$\frac{V\Delta t_{ED}}{2} \left( \sum_{m=1}^{i-1} C'_m + \frac{1}{V^2} \sum_{m=1, m \neq i}^{j-1} \beta'_{im} \right) < r_1 \leq \frac{V\Delta t_{ED}}{2} \left( \sum_{m=1}^{i-1} C'_m + \frac{1}{V^2} \sum_{m=1, m \neq i}^j \beta'_{im} \right), \tag{9}$$

is satisfied. When the acceptance-rejection method is used by the event-driven MC method, simulation particle  $i$  and  $j$  undergo a coagulation event if a random number is less than the value  $\beta'_{ij} / \max_{v_k, v_m}(\beta'_{km})$ , where  $i$  and  $j$  are randomly chosen from the simulation particle population. This procedure is repeated until a particle pair is accepted.

In time-driven MC, each simulation particle is examined successively to determine whether the particle coagulates within  $\Delta t_{TD}$  and  $V$ , and, if the particle coagulates, who is its partner. As for simulation particle  $i$ , the probability of a coagulation event of  $i$  taking place within  $\Delta t_{TD}$  and  $V$  is an exponentially distributed random variable, that is:

$$P'_{E,i}(\Delta t_{TD}) = 1 - \exp(-VC'_i\Delta t_{TD}/2). \tag{10}$$

Once a random number  $r_2$  is less than  $P'_{E,i}(\Delta t_{TD})$ ,  $i$  is allowed to coagulate. Its partner  $j$  is then found based on the probability  $P'_{ij}$ . In the cumulative probabilities method, the partner  $j$  is selected by means of the random number  $r_2$  from the condition:

$$\sum_{k=1}^{j-1} P'_{ik} \leq r_2 \leq \sum_{k=1}^j P'_{ik}, \quad \text{where } P'_{ij} = \beta'_{ij} / \sum_{k=1, k \neq i}^{N_{st}} \beta'_{ik}; \quad j, k \in [1, N_{st}]. \tag{11}$$

In the acceptance-rejection method, a randomly selected particle  $j$  is accepted as coagulation partner of  $i$  if the following condition is met:

$$r_3 \leq \beta'_{ij} / \max_{v_k, v_m}(\beta'_{km}). \tag{12}$$

Random numbers  $r_3$  are generated and this condition is checked until a particle pair is accepted.

### 2.2.3. The treatment of a coagulation event

At the end of a time step, all of the selected coagulation event(s) is(are) implemented according to the probabilistic coagulation rule. As for the  $i$ - $j$  coagulation event, two new simulation particles having new weights and/or volumes replace the “old” particles  $i$  and  $j$ . This is shown in Fig. 1 and is formulated by Eq. (13):

$$\begin{aligned} \text{if } w_i \neq w_j, & \begin{cases} w_i^* = \max(w_i, w_j) - \min(w_i, w_j); v_i^* = v_k |_{w_k = \max(w_i, w_j)}, \\ w_j^* = \min(w_i, w_j); v_j^* = v_i + v_j, \end{cases} \\ \text{if } w_i = w_j, & \begin{cases} w_i^* = w_i/2; v_i^* = v_i + v_j, \\ w_j^* = w_j/2; v_j^* = v_i + v_j, \end{cases} \end{aligned} \tag{13}$$

where the asterisk indicates a new value of weight or volume after the coagulation event.

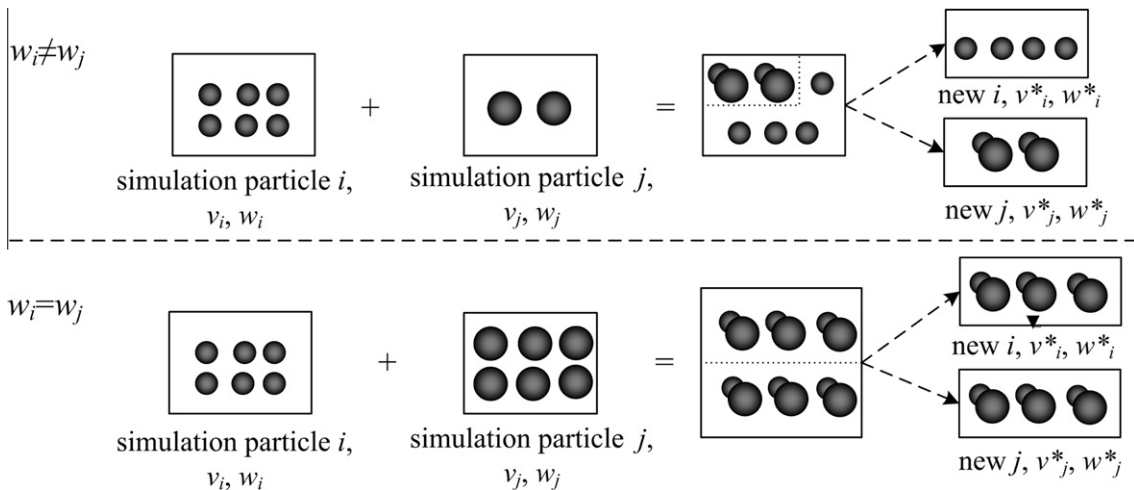


Fig. 1. Treating a coagulation event under the probabilistic coagulation rule.

The new unified differentially weighted MC method simultaneously has the characteristics of constant volume and constant number. Depending on the particulars of the problem, either the time-driven mode or event-driven mode can be selected. Generally speaking, the event-driven version is more accurate because events are fully uncoupled among different time steps, while the time-driven mode is faster because many more events are simulated within one time step. Furthermore, it is emphasized that the popular equally weighted MCs such as the stepwise constant volume method [18,29] (an event-driven MC) and the time-driven DSMC [30] are special versions of the differentially weighted MC. In the following text, we refer only to the differentially weighted MC, where neither the event-driven mode nor the time-driven mode is emphasized.

### 2.3. Composition-dependent weighting scheme

In the differentially weighted MC for two-component systems, the two individual component distributions,  $n_x(v_x, t)$  and  $n_y(v_y, t)$ , are divided into intervals by laws which can be freely adapted to the problems to be solved. Fig. 2 shows a schematic of the two-dimensional internal variable space of the population of simulation particles. One grid point  $(p, q)$  in the  $v_x$ - $v_y$  plane represents a state  $(v_{x,p}, v_{y,q})$  of particles having  $x$ -component volumes between  $v_{x,p}^-$  and  $v_{x,p}^+$  and  $y$ -component volumes between  $v_{y,q}^-$  and  $v_{y,q}^+$ ; the height of the cube located at the grid point  $(p, q)$  represents the number of real particles with state  $(v_{x,p}, v_{y,q})$ ,  $N(v_{x,p}, v_{y,q})$ . Particles at the same grid point of the two-dimensional space are considered to have similar dynamic behavior and are represented by a certain number of weighted simulation particles. The mean weight of simulation particles located at the grid point  $(p, q)$  is thus calculated as:

$$\bar{w}_{pq}(v_{x,p}, v_{y,q}) = N(v_{x,p}, v_{y,q})/N_s(v_{x,p}, v_{y,q}), \quad (14)$$

where  $N_s(v_{x,p}, v_{y,q})$  is the number of simulation particles located at the grid point  $(p, q)$ . The number of simulation particles at each grid point must be sufficient to minimize statistical noise. In this paper,  $N_s$  is prescribed to be more than a fixed minimum number  $N_{s,\min}$  but less than a maximum number  $N_{s,\max}$ . Grid points where the number density of real particles is high can thus be designated to have numbers of simulation particles having larger mean weight values than grid points where the number density is low.

### 2.4. Composition-dependent shift action

Based on the component-dependent weighting scheme, the differentially weighted MC method described above can be utilized in the simulation of two-component coagulation processes. Since the history of each simulation particle can be retained, the extension of the MC method from mono-component systems to multi-component systems is in theory only to assign multiple internal variables (the volume of different chemical components in this paper) to individual simulation particles. Although this direct extension does not increase the complexity of MC code, neither does it specify how the sim-

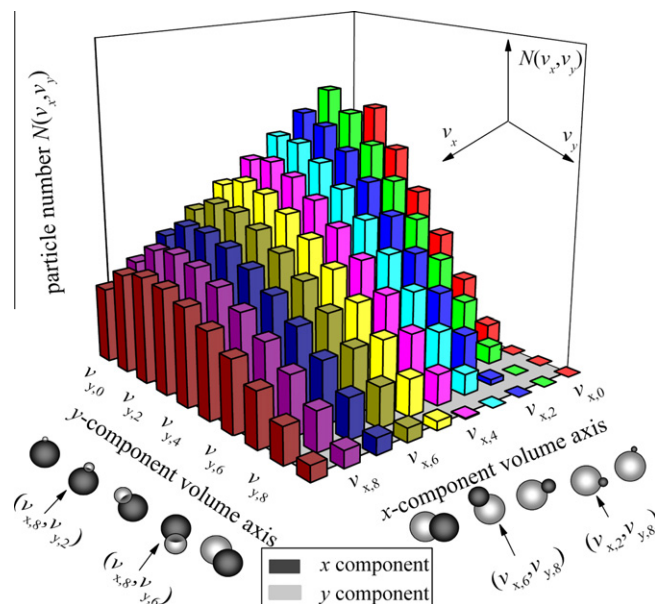


Fig. 2. Schematic illustration of the discretized two-dimensional internal variable space of simulation particle population.



ulation particles are distributed over the multi-dimensional space of internal variables. It is well known that the statistical error in the distribution function of one chemical composition, for example  $x$ -component, depends heavily on the square root of  $N_s(v_{x,p})$ , where  $N_s(v_{x,p})$  is the number of simulation particles having  $x$ -component with volumes between  $v_{x,p}^-$  and  $v_{x,p}^+$ . It is therefore necessary to specify a minimum number of simulation particles in each size interval of each component space, especially in less-populated regions, during the simulation of the coagulation process. At the same time, there are many simulation particles in some size intervals of component space where the number concentrations are very high. In view of the modest improvement in statistical precision and excessive computational cost, too many simulation particles in a size interval of component space are unnecessary. It is therefore more efficient to specify a maximum number of simulation particles in each size interval of component space. In summary, the simulation particles should be distributed over the two-dimensional space of two compositions as homogeneously as possible during the two-component coagulation simulation by some additional action. We have proposed the “shift” action in differentially weighted MC methods for mono-variate systems to reduce statistical noise [25]. The shift action is extended to the two-component coagulation simulation in the following way:

When certain conditions are reached, for example when the number concentration of real particles is halved, the shift action is performed, which restricts the number of simulation particles in predefined size intervals of each component space to within these prescribed bounds (between  $N_{s,\min}$  and  $N_{s,\max}$ ). First, the distribution of each component is sectionalized by some prescribed laws, and then the number of simulation particles in the chosen intervals of each component space is counted. In this paper, as for cases of initially discrete component distribution, the used size intervals of  $x$ -component space are of the following general structure:  $v_{x,h} = h \times v_{x,\min}$ ,  $h = 1, \dots, 20$ ;  $v_{x,h} = f_s v_{x,h-1}$ ,  $h = 21, \dots, 100$ , and the section spacing factor  $f_s$  depends on the maximum volume of  $x$ -component at the time instance and has an initial value of 1.08. The distribution of the other component is also sectionalized in a similar manner; as for cases of initial polydisperse distribution, each component volume is sectionalized into 100 size intervals between the minimum and maximum volumes by means of a logarithmic law. The number of simulation particles in each size interval of each component space is required to exceed a prescribed minimum  $N_{s,\min}$  (for example 100 in this paper). A simple example is used to illustrate the action. Simulation particle A has an  $x$ -component volume  $v_{x,A}$ , a  $y$ -component volume  $v_{y,A}$ , a weight  $w_A$ , and a total volume ( $v_{x,A} + v_{y,A}$ ). The particle is located at the grid point  $(p, q)$  of the two-component space, i.e.,  $v_{x,p}^- \leq v_{x,A} \leq v_{x,p}^+$  and  $v_{y,q}^- \leq v_{y,A} \leq v_{y,q}^+$ . The numbers of simulation particles in size interval  $p$  of  $x$ -component space and size interval  $q$  of  $y$ -component space are  $N_{sx,p}$  and  $N_{sy,q}$ , respectively. If  $\min(N_{sx,p}, N_{sy,q}) < N_{s,\min}$ , the simulation particle A is equally split into new simulation particles with an integer number  $[N_{f,\min}/\min(N_{sx,p}, N_{sy,q})]$ . These new particles have the same internal variables as their parent particle A and a weight of  $w_A/[N_{s,\min}/\min(N_{sx,p}, N_{sy,q})]$ . One daughter particle replaces the position of its parent particle A, and other daughter particles are added to the array of simulation particles. The action does not change the compositional distributions, and it also conserves the history of the particles but at the cost of more simulation particles.

If  $N_{sx,p}$  or  $N_{sy,q}$  is greater than a prescribed maximum  $N_{s,\max}$  (1000 in this paper), each simulation particle in the grid point  $(p, q)$  can be randomly removed with a probability of  $[\max(N_{sx,p}, N_{sy,q}) - N_{s,\max}]/\max(N_{sx,p}, N_{sy,q})$ . In this paper, the removal probability is prescribed to be less than 0.5 in order to avoid intense disturbance of simulation particle population. A random process is used to decide whether simulation particle B is removed or not. If it is removed, the open position is taken by the last particle in the simulation particle array. If not, the number weight of simulation particle B is corrected by a multiple factor  $\max(N_{sx,p}, N_{sy,q})/N_{s,\max}$ . If the total number of simulation particles is large enough, the random removal action does not lead to a change in the distribution of each chemical composition or the joint distribution of two-components (on average). As a consequence, the removal action results in less simulation particles.

The action described above shifts some simulation particles from densely-populated regions of the two-dimensional component space to less-populated regions by splitting some simulation particles in less-populated regions into more simulation particles and randomly removing some simulation particles in densely-populated regions from the simulation. It is clear that the shift action can only be used by the differentially weighted MC method, since the action necessitates consideration (and recalculation) of the individual weights. The shift action overcomes the drawback of a stochastic approach as far as possible, and at the same time the computational cost can be limited.

## 2.5. Smart bookkeeping technique

The computational cost of MC can further be reduced by the smart bookkeeping technique that is described in Ref. [25]. The key idea of the bookkeeping technique is to update the total coagulation rate of each simulation particle after each time step. Since there are only a few portions of simulation particles in time-driven mode or two simulation particles in event-driven mode related to coagulation event(s) within a time step, the total coagulation rate of a non-coagulated simulation particle after the time step can be calculated by only updating the normalized kernels between the non-coagulated simulation particles and the coagulated simulation particles (their weights and volumes may change according to Eq. (13)). Double counting over all simulation particles is thus avoided during the simulation itself and in fact only has to be performed at the very first time step. The smart bookkeeping technique in the differentially weighted MC is similar in nature to the bookkeeping technique proposed by Laurenzi et al. [16]. By using an “aggregation table”, the latter significantly improves the computational efficiency of the event-driven MC for simulating multi-component coagulation processes.

### 3. Numerical test cases

In this section, the performance of the differentially weighted MC method is evaluated by testing it for two ideal cases for which analytical solutions exist: an initially monodisperse distribution of each component and an initially polydisperse distribution of each component. For these initial cases, analytical solutions for the two-component coagulation processes are available in the case of simple coagulation kernels (constant [7,16,31], sum [16,32], and product [16]). The numerical results from our MC method will be compared with the corresponding analytical solutions, showing that the differentially weighting scheme and the component-dependent shift action are necessary to obtain an accurate MC solution for two-component coagulation.

#### 3.1. Two-component coagulation of two initial monodisperse components, sum kernel

The coagulation process starts from two individual monodisperse compositional distributions, that is, 10,000 particles fully consisting of  $x$ -component and 20,000 particles fully consisting of  $y$ -component. For the theoretical and unrealistic case, the initial volume of all particles is  $v_0 = v_{x,0} = v_{y,0} = 1$  (dimensionless), and the computational domain  $V$  is unit volume (dimensionless). The sum (additive) coagulation kernel considered here has the form  $\beta(v_i, v_j) = \beta_{ij} = B(v_i + v_j)$ , where  $B = 1$ . The characteristic coagulation time is defined as  $\tau_{coag} = 1/(Bv_0N_0) = 3.33 \times 10^{-5}$  (dimensionless).

Two kinds of MC methods will be compared: the differentially weighted MC method and the non-weighted MC method. The non-weighted MC method, which is described in Ref. [30], is de facto a special version of the differentially weighted one. The non-weighted MC can keep the number of simulation particles constant in each step; however it does not allow the shift action to be adopted. The non-weighted MC can be considered as a typical representative of MC methods available in the open literature. The non-weighted MC starts with 20,000 simulation particles and ends with around 10,900 simulation particles due to number depletion caused by the coagulation process; the differentially weighted MC starts with 1000 simulation particles and ends with 9300 simulation particles as a direct result of the component-dependent shift action. The CPU time consumed by the non-weighted and differentially weighted methods for one MC simulation is around 144 s and 214 s, respectively on a computer equipped with an Inter (R) Core (TM) 2 Quad CPU Q9300 @ 2.50 GHz and 4 GB memory. The non-weighted MC is faster (1) because the non-weighted MC is factually based on the full coagulation rule, i.e., each real particle from coagulated simulation particles participates in the real coagulation process. Under the probabilistic coagulation rule, however, only some of the real particles coagulate: in other words, there are some “null” real coagulation events. The non-weighted MC based on the full coagulation rule thus evolves faster than the differentially weighted MC based on the probabilistic coagulation rule; and (2) because the shift action adopted by the differentially weighted MC consumes some CPU time. The differentially weighted MC gives something (computational efficiency) and gets something (computational precision) in return.

The moments of the number density function  $n(v_x, v_y, t)$  are defined as:

$$M_{ij}(t) = \int_0^\infty \int_0^\infty v_x^i v_y^j n(v_x, v_y, t) dv_x dv_y, \quad (15)$$

and the evolution of the moments is shown in Fig. 3. The numerical results from the non-weighted and differentially weighted MC methods (see Fig. 3(a)) agree with the analytical solutions [16]. However, there are subtle differences in the behavior of  $M_{1,1}$  at short times ( $t < 0.1 \tau_{coag}$ ) from the analytical solutions and MC solutions. In fact, analytical solutions from the deterministic equation (1) describe the average behavior of the two-component coagulation, while MC simulations represent a single experiment having innate fluctuation; and deterministic solutions are exactly valid only for an “infinite” system [16], while 30,000 real particles and less simulation particles are insufficient to simulate the behavior of mixing between components (like  $M_{1,1}$ ) in an infinite system.

From the calculated moments (shown in Fig. 3(a)) and their relative errors with respect to analytical solutions (shown in Fig. 3(b)), it is difficult to evaluate the performance of different MC methods. In order to quantify numerical errors from the different MC methods, we calculated the root mean squared error (RMSE) of the moments for 10 MC simulations with respect to the analytical solution as follows:

$$\sigma_{M_{ij}}(t) = \sqrt{\frac{1}{Q} \sum_{k=1}^Q \left( \left[ \frac{M_{ij}^{MC(k)}(t) - M_{ij}^{AS}(t)}{M_{ij}^{AS}(t)} \right]^2 \right)}, \quad (16)$$

where  $Q$  is the number of MC repetitions ( $Q = 10$ ); the superscript “AS” represents the analytical solution and “MC ( $k$ )” means the numerical result of the  $k$ th MC simulation. These errors as a function of the normalized time are plotted in Fig. 4. It is clear that the solid lines (representing the differentially weighted method) on the whole are below the dotted lines (representing the non-weighted method). The differentially weighted method is more accurate than the non-weighted method, especially for these higher-order moments (like  $M_{1,1}$ ,  $M_{0,2}$ ,  $M_{2,0}$ ) when  $t > \tau_{coag}$ , which should be attributed to the fact that these equally weighted simulation particles are not capable of representing the increasingly polydispersed and non-isotropic compositional distributions as time evolves.

Even when  $t < \tau_{coag}$ , the differentially weighted method predicts the two-component coagulation process more accurately than the non-weighted method, although this is not as evident when comparing the moments and their relative error.



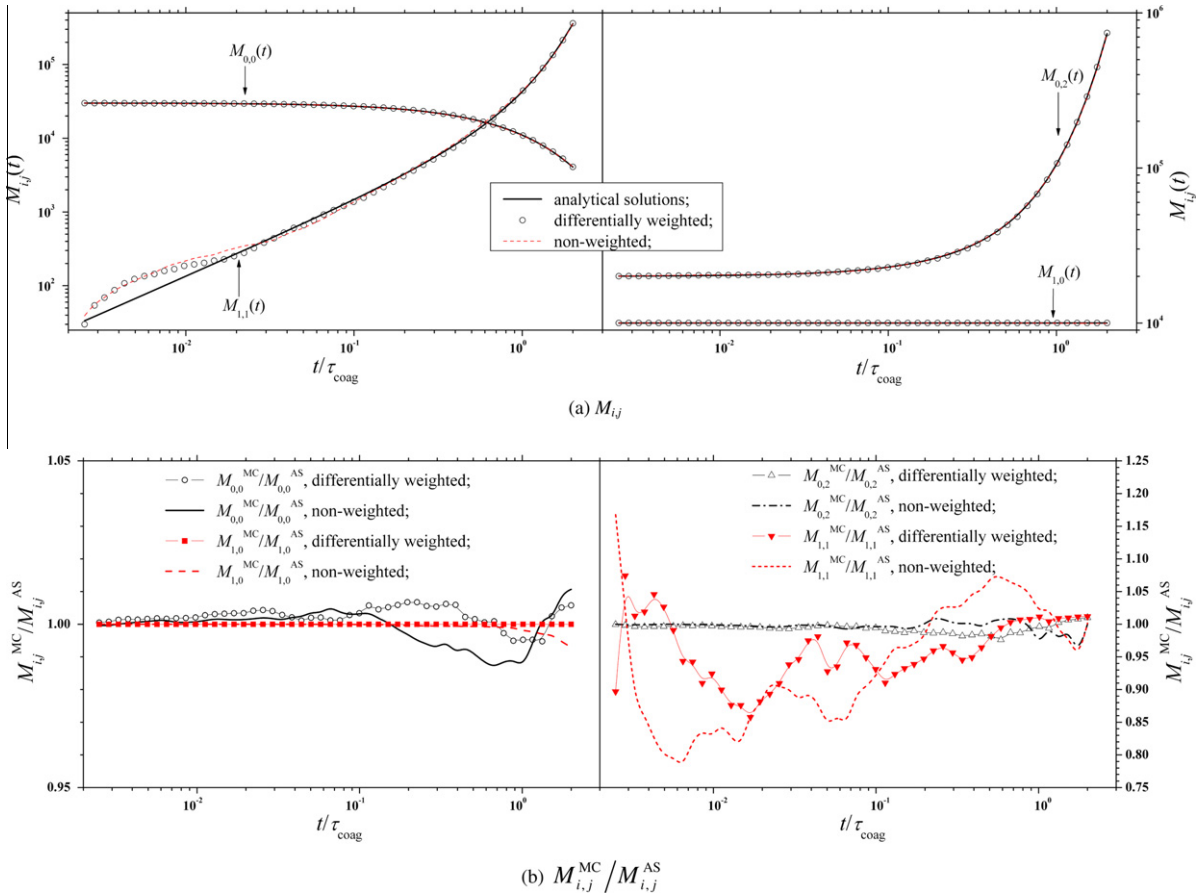


**Fig. 3.** Two initially monodisperse distributions in the case of a sum kernel: comparison between the analytical solutions [16] and numerical results from two MC methods for the evolution of the moments of two-component distribution. (a)  $M_{ij}$ ; (b)  $M_{ij}^{\text{MC}}/M_{ij}^{\text{AS}}$  the ratio, where the superscript “MC” represents the numerical result of the two MC methods and “AS” the analytical solution.

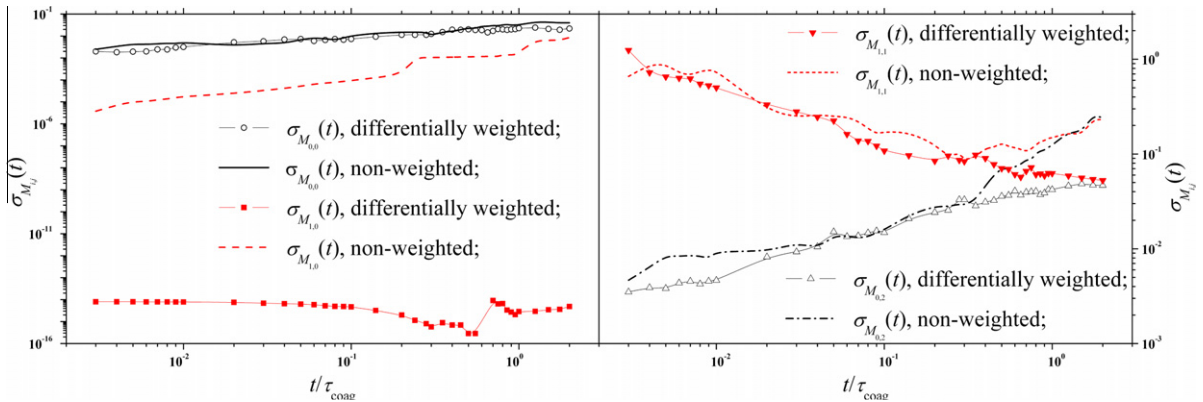


**Fig. 4.** Two initially monodisperse distributions in the case of a sum kernel: root mean squared errors of several moments to the analytical solution from 10 MC simulations.

Exemplary particle size distributions, Fig. 5, show that the non-weighted method exhibits good performance only in the densely-populated regions. However, it exhibits greater fluctuations in less-frequently encountered particles (for example larger aggregates having nonisotropic compositional distribution). By contrast, the differentially weighted method is capable of tracking the largest aggregates which have very low probabilities of occurrence.

To evaluate the relative performance of the MC methods with respect to the compositional and size distribution on a quantitative basis, we also computed the standard deviations of distributions as follows:

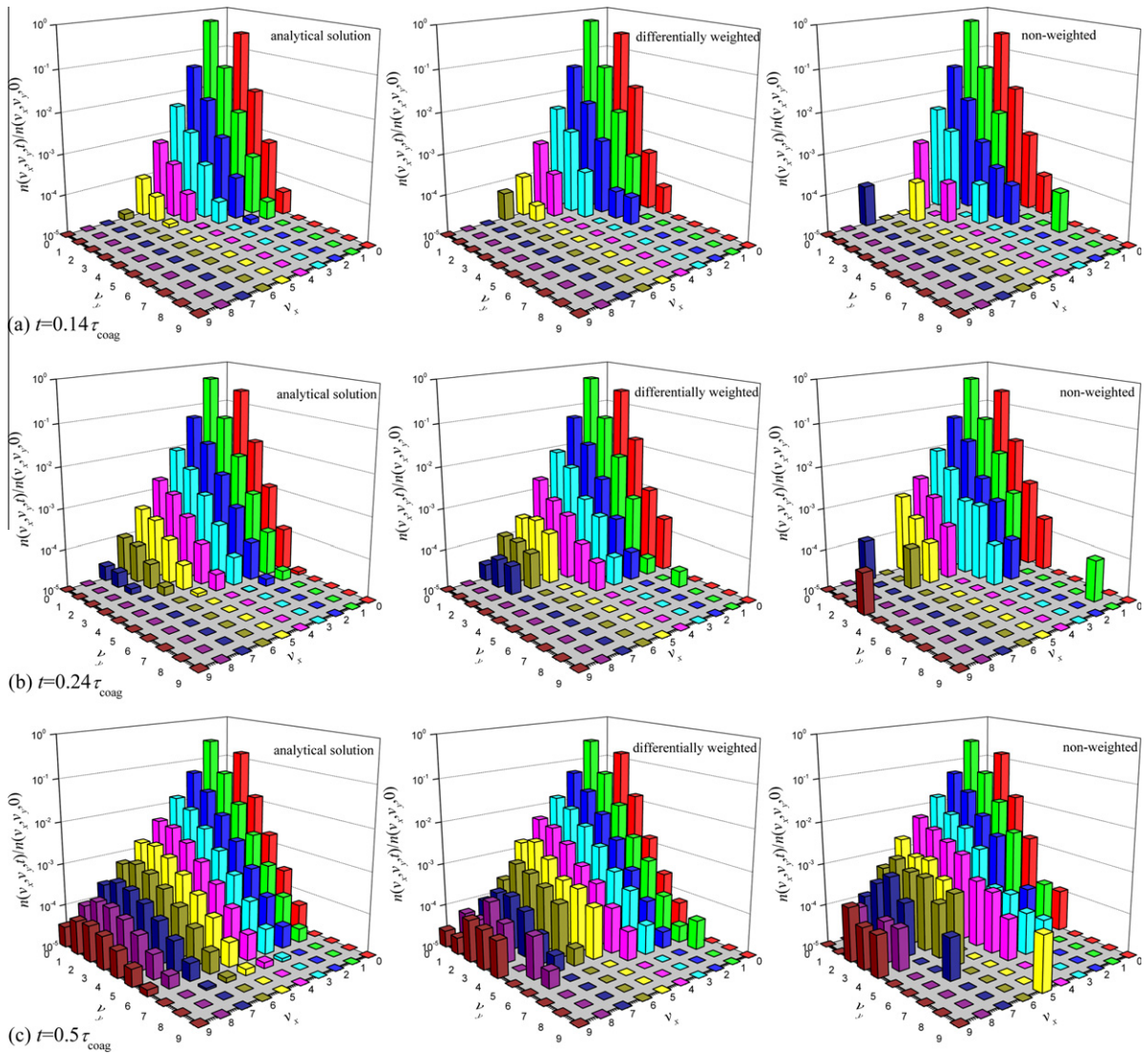


Fig. 5. Normalized particle size distribution  $n(x,y,t)/n(x,y,0)$  at (a)  $t = 0.14\tau_{coag}$  (b)  $t = 0.24\tau_{coag}$  (c)  $t = 0.5\tau_{coag}$ .

$$\begin{aligned}
 \sigma_n(t) &= \sqrt{\frac{1}{Q} \sum_{k=1}^Q \zeta_n^{(k)}(t)}; \\
 \zeta_{n_{x+y}}^{(k)}(t) &= \frac{1}{S} \sum_{h=1}^S \left[ \frac{n_{x+y}^{MC(k)}(v_h, t) - n_{x+y}^{AS}(v_h, t)}{\max\{n_{x+y}^{MC(k)}(v_h, t), n_{x+y}^{AS}(v_h, t)\}} \right]^2; \\
 \zeta_{n_x(v_x)}^{(k)}(t) &= \frac{1}{S_x} \sum_{p=1}^{S_x} \left[ \frac{n_x^{MC(k)}(v_{x,p}, t) - n_x^{AS}(v_{x,p}, t)}{\max\{n_x^{MC(k)}(v_{x,p}, t), n_x^{AS}(v_{x,p}, t)\}} \right]^2; \\
 \zeta_{n_y(v_y)}^{(k)}(t) &= \frac{1}{S_y} \sum_{q=1}^{S_y} \left[ \frac{n_y^{MC(k)}(v_{y,q}, t) - n_y^{AS}(v_{y,q}, t)}{\max\{n_y^{MC(k)}(v_{y,q}, t), n_y^{AS}(v_{y,q}, t)\}} \right]^2; \\
 \zeta_{n(v_x, v_y)}^{(k)}(t) &= \frac{1}{S_x S_y} \sum_{p=1}^{S_x} \sum_{q=1}^{S_y} \left[ \frac{n^{MC(k)}(v_{x,p}, v_{y,q}, t) - n^{AS}(v_{x,p}, v_{y,q}, t)}{\max\{n^{MC(k)}(v_{x,p}, v_{y,q}, t), n^{AS}(v_{x,p}, v_{y,q}, t)\}} \right]^2;
 \end{aligned} \tag{17}$$

where  $n_{x+y}(v)$  is the particle size distribution function,  $n_x(v_x)$  is the  $x$ -component distribution function and  $n_y(v_y)$  is the  $y$ -component distribution function;  $S$  is the number of size intervals in particle size space,  $S_x$  is the number of size intervals in  $x$ -component space and  $S_y$  in  $y$ -component space. The relative errors of distribution functions are normalized by the maximum value of either the MC results or the analytical solution because in some size intervals MC results differ greatly from analytical solutions, which would mask the overall error too heavily. In this case, the standard deviations of distributions in particle size space ( $v_0, 20v_0$ ) and bi-component space ( $v_{x,0}, 10v_{x,0}$ )  $\times$  ( $v_{y,0}, 10v_{y,0}$ ) are shown in Fig. 6. When  $t < 0.1\tau_{coag}$ , it is difficult to distinguish the advantages and disadvantages of the two MC methods for distribution functions; however, it is easy to determine from the quantitative standard deviations of distribution functions that the differentially weighted method simulates size distribution and bi-component distribution more accurately when  $t > 0.1\tau_{coag}$ . The good performance of the differentially weighted method is directly due to the differentially weighting scheme and the composition-dependent shift action, which are capable of distributing a limited number of simulation particles over the simulated multi-dimensional space as homogeneously as possible. Note that the better precision of the differentially weighted MC is achieved under the condition that its simulation particle number is always less at same time instants than the number of simulation particles in the non-weighted method.

### 3.2. Two-component coagulation of two initial polydispersed components, constant kernel

In this case the initial number density function satisfies:

$$n(v_x, v_y, 0) = \frac{N_0}{v_{x,0}v_{y,0}} \exp\left(-\frac{v_x}{v_{x,0}} - \frac{v_y}{v_{y,0}}\right), \tag{18}$$

where  $N_0$  is the total number concentration of real particles ( $10^{10}$  in this simulation, dimensionless);  $v_{x,0}$  and  $v_{y,0}$  are the initial geometric mean volume of  $x$ -component and  $y$ -component in a particle ( $v_{x,0} = v_{y,0} = 0.5$  in this simulation, dimensionless). The coagulation kernel is size-independent,  $\beta(v_i, v_j) = \beta_{ij} = A = 10^{-10}$  (dimensionless). In this case, two versions of the differentially weighted MC are numerically implemented: the MC that adopts the shift action (shift MC) and the MC that does not adopt the shift action (no-shift MC). The two MC simulations start with 10,204 simulation particles. The no-shift MC keeps the simulation particle number constant during the simulation, however the shift MC will increase the simulation particle number up to around 35,000 by the end of coagulation process ( $t = 10,000\tau_{coag}$ , where the dimensionless  $\tau_{coag} = 1/(AN_0) = 1$ ).

As for the moments of  $n(v_x, v_y, t)$ , the agreement between the results of either MC and analytical solutions is very good. At first sight, the evolution of the three moments ( $M_{0,0}, M_{0,1}, M_{1,1}$ ) along with  $t$  is identical to the analytical solution as shown in Fig. 7(a). However, when comparing the relative error of these moments (Fig. 7(b)), the error in the shift MC method is greater than that in the no-shift MC method. In the shift action, some simulation particles are randomly removed in order to restrict the simulation particle number in each size interval of each component space to within prescribed bounds, which results in small deviations in these moments.

The root mean squared errors of these moments for ten MC simulations as a function of time with respect to the analytical solution are shown in Fig. 8. In the early stage of MC simulations, the two versions of the differentially weighted method show similar accuracy for these moments because the first shift action occurs at about  $t = 2.12\tau_{coag}$ . After that, the shift MC shows increasing numerical errors because the shift action continuously introduces random noise to the population of simulation particles.

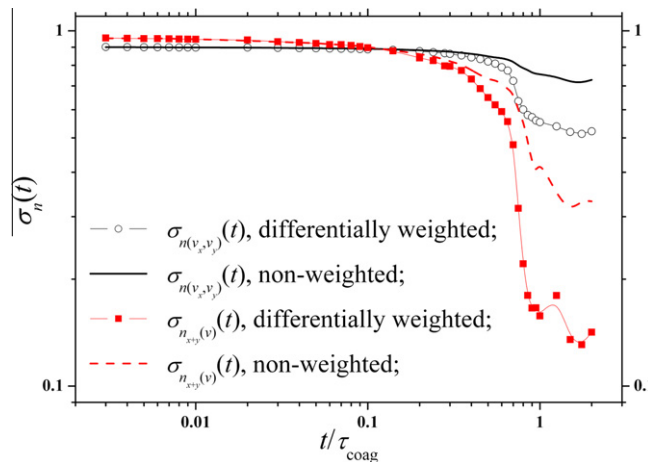


Fig. 6. Two initially monodisperse distributions in the case of a sum kernel: standard deviations of the particle size distribution and the combined compositional distribution from 10 MC simulations.

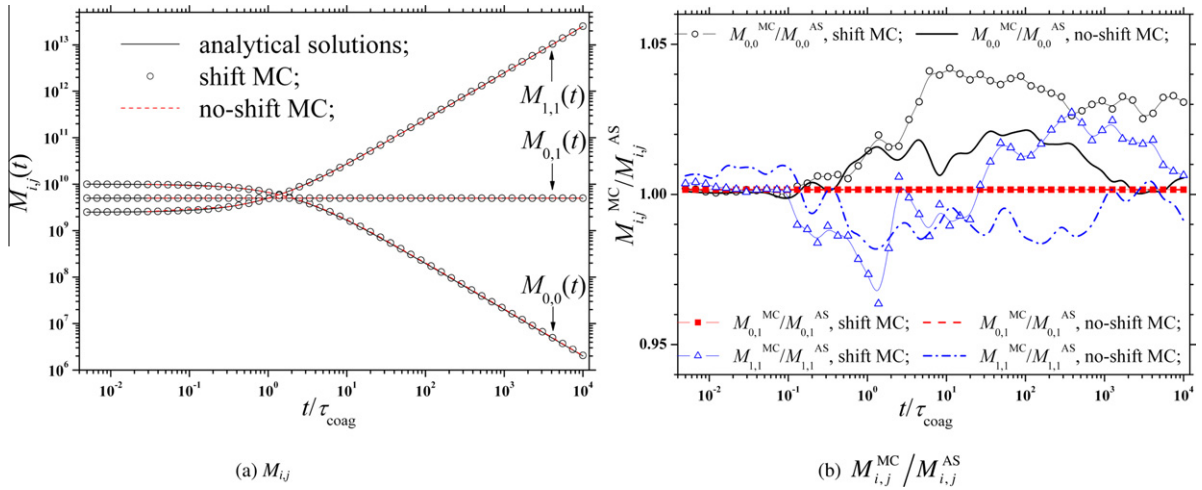


Fig. 7. Two initial polydispersed components in the case of a constant kernel: comparison between the analytical solutions [7] and numerical results from two MC methods for the evolution of the moments. (a)  $M_{i,j}$ ; (b) the ratio  $M_{i,j}^{\text{MC}}/M_{i,j}^{\text{AS}}$ .

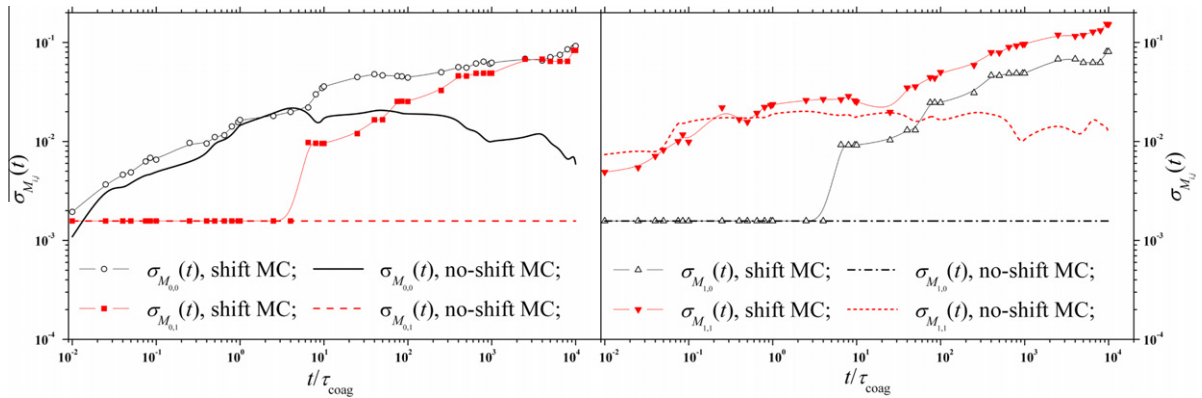


Fig. 8. Two initial polydispersed components in the case of a constant kernel: root mean squared errors of several moments from 10 MC simulations.

Although the shift action adopted in the differentially weighted MC method apparently does not help to improve the accuracy of the global moments, the method is very useful for obtaining more exact results in the less-populated regions in the compositional distribution. As shown in Fig. 9, the shift MC method is capable of predicting the compositional

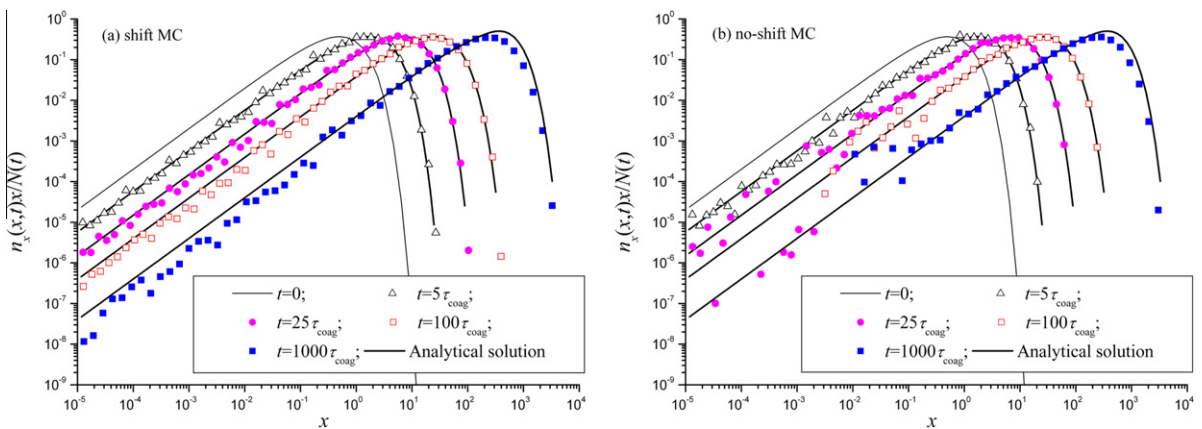
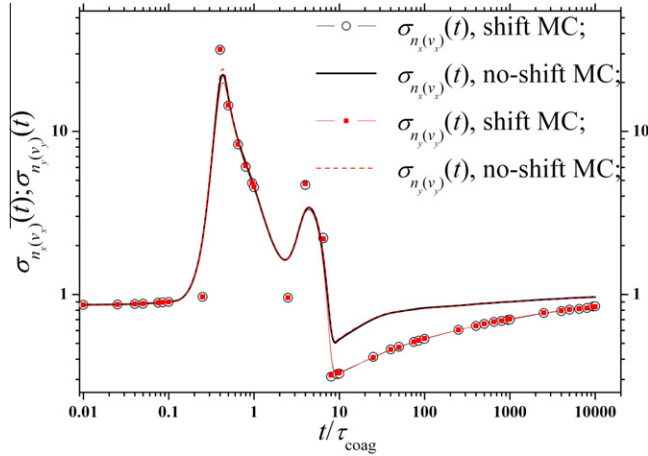


Fig. 9. The time-dependent-component distribution for two initial polydispersed components in the case of a constant kernel: comparison between the analytical solutions [7] and numerical results from (a) the differentially weighted MC that adopts the shift action; and (b) the differentially weighted MC that does not adopt the shift action.



distributions even when the degree of coagulation is very high (in Fig. 9(a)). The four time instants,  $t = 5\tau_{coag}$ ,  $25\tau_{coag}$ ,  $100\tau_{coag}$  and  $1000\tau_{coag}$ , correspond to the coagulation degree of around 70.48%, 92.35%, 97.98% and 99.80%, respectively. It is clear that the no-shift MC method leads to larger statistical noise for these less-populated component regions (for example,



**Fig. 10.** Standard deviations of the particle size distribution and the combined compositional distribution from 10 MC simulations for two initial polydispersed components in the case of a constant kernel.

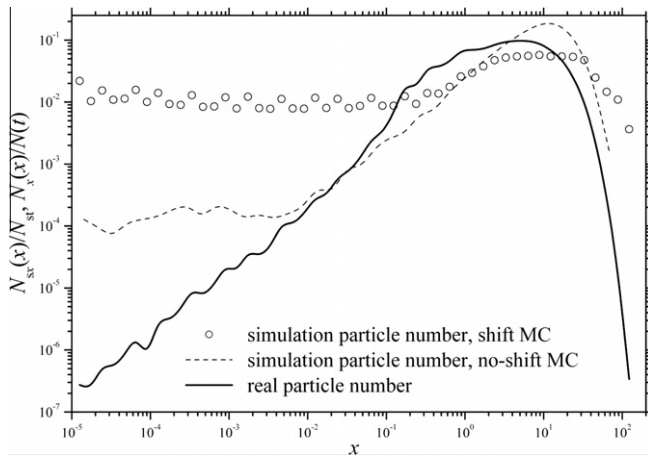


**Fig. 11.** Normalized simulation and real particle numbers,  $N_{sx}(v_x)/N_{st}$  and  $N_x v_x / N(t)$  at  $t = 25\tau_{coag}$ .

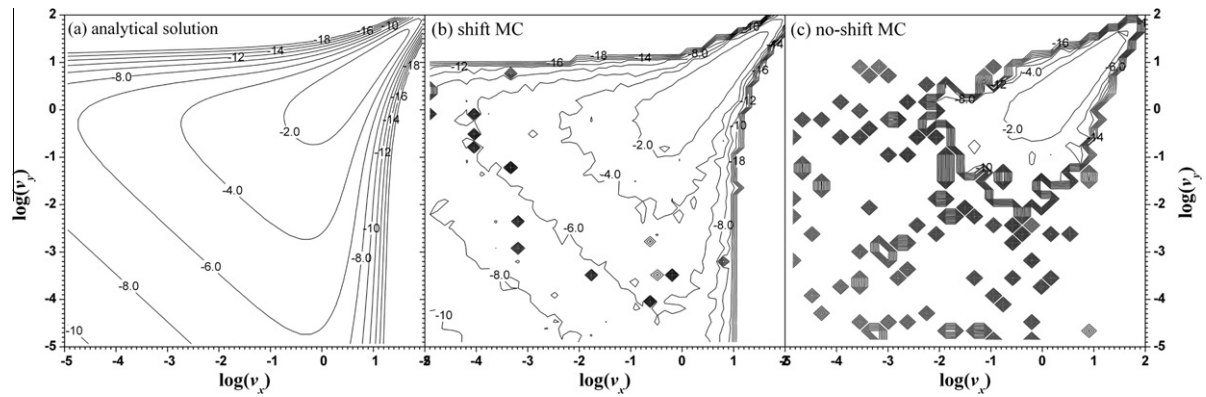


**Fig. 12.** Contour plot of the logarithm of the normalized two-dimensional compositional distribution function,  $\log_{10}[n(v_x, v_y, t)/n(v_x, v_y, 0)]$ , at  $t = 25\tau_{coag}$  (a) analytical solution [7]; (b) the differentially weighted MC method that adopts the shift action; (c) the differentially weighted MC method that does not adopt the shift action.



$x < 0.1$ ) when the system has experienced long-term evolution ( $t > 5\tau_{coag}$ ). The standard deviations of compositional distributions, which are shown in Fig. 10, further prove this point. When  $t < 5\tau_{coag}$ , the shift and no-shift MCs show similar accuracy in compositional distribution; however, the performance difference between two MCs begins to appear when  $t > 5\tau_{coag}$ . The shift MC exhibits a smaller standard deviation of compositional distributions when  $t > 5\tau_{coag}$ . In fact, the better performance of the shift MC method is directly ascribed to the fact that the simulation particles are distributed over the two-dimensional component distribution during the simulation as homogeneously as possible. Fig. 11 shows the composition-dependent simulation particle number at  $t = 25\tau_{coag}$ . It is found that the shift MC method still assigns appropriate numbers of simulation particles to represent these less-populated regions (the two edges of compositional distributions). By contrast, if the simulation particles are freely evolved (in the no-shift MC method), most of the simulation particles are still distributed in these densely-populated regions where the number density is high. The shift action also supplies enough information for a two-dimension contour plot of the component distribution to be calculated (Fig. 12), whereas the non-shift method does not lead to an acceptable contour plot.

#### 4. Conclusions

An intrinsic characteristic of the direct simulation Monte Carlo method that has contributed to its increased applicability in complex dispersed systems is its ability to deal with multivariate problems in a simple and straightforward manner. As for multi-component coagulation processes, the available MC methods which only assign multiple internal variables to individual simulation particles have numerical difficulties such as large statistical noise. At the same time, however, MC methods which treat multi-component coagulation as chemical reactions of many species overcome these numerical difficulties at the cost of increasing complexity. In this paper, a robust, accurate and smart stochastic algorithm is introduced which exhibits an optimal combination of high numerical accuracy and low computational effort. It is based on a new generalized differentially weighted MC method for monovariate systems, which unifies event-driven mode and time-driven mode, has the characteristics of constant volume and constant number (between two shift actions), and is capable of using so-called smart bookkeeping to improve computational efficiency. The new distinguishing feature of the differentially weighted MC for bi-component coagulation is the so-called component-dependent shift action, which restricts the number of simulation particles for each size interval of each component space to within prescribed bounds during simulation. From a comparison of the differentially weighted and non-weighted MCs with a benchmark solution (two initially monodisperse distributions in the case of a sum kernel), it is found that the differentially weighted MC shows smaller errors for the moments of compositional distributions in the more advanced stages of coagulation and simulates size distribution and compositional distributions more accurately even in the initial stage of coagulation, while it performs less efficiently than the non-weighted MC. Furthermore, comparison between an analytical solution and numerical results from the differentially weighted method either with or without the shift action showed that, although it does not improve the accuracy of global distribution properties such as moments, the shift action is necessary in order to obtain information about sparsely populated regions of the distribution function.

#### Acknowledgments

H. Zhao was supported with funds from “The National Natural Science Foundation of China” (20606015, 50876037 and 50721005), “Program for New Century Excellent Talents in University” (NECT-10-0395), “National Key Basic Research and Development Program” (2010CB227004), “Fok Ying Tung Education Foundation” (114017) and “Alexander von Humboldt Foundation”. F.E. Kruis acknowledges the financial support of the Deutsche Forschungsgemeinschaft (DFG) in the framework of the collaborative research program “Nanoparticles from the gas phase: formation, structure, properties” (SFB 445).

#### References

- [1] S.K. Friedlander, *Smoke, Dust and Haze: Fundamentals of Aerosol Dynamics*, second ed., Oxford University Press, New York, Oxford, 2000.
- [2] C. Kiparissides, Polymerization reactor modeling: a review of recent developments and future directions, *Chemical Engineering Science* 51 (10) (1996) 1637–1659.
- [3] J.D. Litster, Scaleup of wet granulation processes: science not art, *Powder Technology* 130 (1–3) (2003) 35–40.
- [4] A. Maisels, F.E. Kruis, H. Fissan, Mixing selectivity in bicomponent, bipolar aggregation, *Journal of Aerosol Science* 33 (1) (2002) 35–49.
- [5] W.P. Linak, J.O.L. Wendt, Toxic metal emissions from incineration: mechanisms and control, *Progress in Energy and Combustion Science* 19 (2) (1993) 145–186.
- [6] J.H. Seinfeld, S.N. Pandis, *Atmospheric Chemistry and Physics*, Wiley-Interscience, New York, 1998.
- [7] A.A. Lushnikov, Evolution of coagulating systems: III. Coagulating mixtures, *Journal of Colloid and Interface Science* 54 (1) (1976) 94–101.
- [8] Y.P. Kim, J.H. Seinfeld, Simulation of multicomponent aerosol condensation by the moving sectional method, *Journal of Colloid and Interface Science* 135 (1) (1990) 185–199.
- [9] Y.P. Kim, J.H. Seinfeld, Simulation of multicomponent aerosol dynamics, *Journal of Colloid and Interface Science* 149 (2) (1992) 425–449.
- [10] R. McGraw, D.L. Wright, Chemically resolved aerosol dynamics for internal mixtures by the quadrature method of moments, *Journal of Aerosol Science* 34 (2003) 189–209.
- [11] H.M. Vale, T.F. McKenna, Solution of the population balance equation for two-component aggregation by an extended fixed pivot technique, *Industrial and Engineering Chemistry Research* 44 (20) (2005) 7885–7891.
- [12] S. Kumar, D. Ramkrishna, On the solution of population balance equations by discretization – I. A fixed pivot technique, *Chemical Engineering Science* 51 (8) (1996) 1311–1332.

- [13] A.H. Alexopoulos, C. Kiparissides, Solution of the bivariate dynamic population balance equation in batch particulate systems: combined aggregation and breakage, *Chemical Engineering Science* 62 (18–20) (2007) 5048–5053.
- [14] S. Qamar, G. Warnecke, Solving population balance equations for two-component aggregation by a finite volume scheme, *Chemical Engineering Science* 62 (3) (2007) 679–693.
- [15] F. Filbet, P. Laurencot, Numerical simulation of the Smoluchowski coagulation equation, *SIAM Journal on Scientific Computing* 25 (6) (2004) 2004–2028.
- [16] I.J. Laurenzi, J.D. Bartels, S.L. Diamond, A general algorithm for exact simulation of multicomponent aggregation processes, *Journal of Computational Physics* 177 (2) (2002) 418–449.
- [17] L. Alfonso, G.B. Raga, D. Baumgardner, Monte Carlo simulations of two-component drop growth by stochastic coalescence, *Atmospheric Chemistry and Physics Discussions* 8 (2) (2008) 7289–7313.
- [18] F.E. Kruijs, A. Maisels, H. Fissan, Direct simulation Monte Carlo method for particle coagulation and aggregation, *AIChE Journal* 46 (9) (2000) 1735–1742.
- [19] V. Saliakas, C. Kotoulas, D. Meimaroglou, C. Kiparissides, Dynamic evolution of the particle size distribution in suspension polymerization reactors: a comparative study on Monte Carlo and sectional grid methods, *The Canadian Journal of Chemical Engineering* 86 (5) (2008) 924–936.
- [20] T. Matsoukas, K. Lee, T. Kim, Mixing of components in two-component aggregation, *AIChE Journal* 52 (9) (2006) 3088–3099.
- [21] K. Lee, T. Kim, P. Rajniak, T. Matsoukas, Compositional distributions in multicomponent aggregation, *Chemical Engineering Science* 63 (5) (2008) 1293–1303.
- [22] Z. Sun, R. Axelbaum, J. Huertas, Monte Carlo simulation of multicomponent aerosols undergoing simultaneous coagulation and condensation, *Aerosol Science and Technology* 38 (10) (2004) 963–971.
- [23] R. Irizarry, Fast Monte Carlo methodology for multivariate particulate systems-I: point ensemble Monte Carlo, *Chemical Engineering Science* 63 (1) (2008) 95–110.
- [24] D.T. Gillespie, A general method for numerically simulating the stochastic time evolution of coupled chemical reactions, *Journal of Computational Physics* 22 (4) (1976) 403–434.
- [25] H. Zhao, F.E. Kruijs, C. Zheng, Reducing statistical noise and extending the size spectrum by applying weighted simulation particles in Monte Carlo simulation of coagulation, *Aerosol Science and Technology* 43 (8) (2009) 781–793.
- [26] H. Zhao, C. Zheng, A new event-driven constant-volume method for solution of the time evolution of particle size distribution, *Journal of Computational Physics* 228 (5) (2009) 1412–1428.
- [27] H.B. Zhao, C.G. Zheng, M.H. Xu, Multi-Monte Carlo approach for general dynamic equation considering simultaneous particle coagulation and breakage, *Powder Technology* 154 (2–3) (2005) 164–178.
- [28] H. Zhao, C. Zheng, Correcting the multi-Monte Carlo method for particle coagulation, *Powder Technology* 193 (1) (2009) 120–123.
- [29] A. Maisels, F.E. Kruijs, H. Fissan, Direct simulation Monte Carlo for simultaneous nucleation, coagulation, and surface growth in dispersed systems, *Chemical Engineering Science* 59 (11) (2004) 2231–2239.
- [30] K. Liffman, A direct simulation Monte-Carlo method for cluster coagulation, *Journal of Computational Physics* 100 (1) (1992) 116–127.
- [31] F.M. Gelbard, J.H. Seinfeld, Coagulation and growth of a multicomponent aerosol, *Journal of Colloid and Interface Science* 63 (3) (1978) 472–479.
- [32] J.M. Fernandez-Diaz, G.J. Gomez-Garcia, Exact solution of Smoluchowski's continuous multi-component equation with an additive kernel, *Europhysics Letters* 78 (5) (2007) 56002.